JOURNAL OF BIOMEDICAL OPTICS 4(3), 368–375 (JULY 1999)

DETECTION OF BREAST LESIONS BY HOLOGRAPHIC INTERFEROMETRY

HyunDae Hong,[†] Daniel B. Sheffer,[‡] and C. William Loughry*
[†]Miami Valley Laboratories, 0N163 (Mail Box 180), 11810 East Miami River Road, Ross, Ohio 45061;
[‡]University of Akron, Department of Biomedical Engineering, Akron, Ohio 44305-0302;
*Biostereometrics Lab/MED-2, Akron City Hospital, 525 E. Market Street, Akron, Ohio 44309

(Paper JBO-200 received Apr. 21, 1998; revised manuscript received Oct. 29, 1998; accepted for publication Apr. 29, 1999.)

ABSTRACT

The holographic interferometry (HI) technique commonly used for nondestructive testing of laminate materials was applied to create fringe contour distortion near the site of indwelling breast lesions. For this medical imaging application, the HI technique was successful in demonstrating abnormal mechanical properties of living tissue. Adequate density and contrast of fringes, crucial factors necessary for analysis of surface deformation of an object, can be made only with an appropriate stressing method. We have applied vibration and mild pressure to the surface of female breasts for the purpose of detecting localized densities and mass alterations of the tissue, which may be indicative of an abnormality of that tissue. Even though each stressing method had both positive and negative aspects, pneumatic pressure was adopted for the present study because it was more suitable for a noninvasive and noncontact breast examination. We also developed a computer based holographic imaging system to precisely control the stressing phase for the pressure and laser triggering so the resultant holograms had manageable fringe density and repeatability. © *1999 Society of Photo-Optical Instrumentation Engineers.* [S1083-3668(99)01303-9]

Keywords breast cancer; holographic interferometry; pulsed ruby laser; fringe pattern.

1 INTRODUCTION

In spite of much research in screening for breast cancer, a reduction in the mortality rate of approximately 22–25 per 100 000 women has not been demonstrated.[1] In fact, this figure has been constant since 1930.[2] Numerous methods of breast cancer screening have been proposed including mammography, thermography, computed tomography (CT), scanning magnetic resonance imaging (MRI), ultrasound, nuclear imaging, and laser transillumination, and yet for a variety of reasons none has proven satisfactory for the task of annually screening the more than 65 000 000 women at risk for breast cancer. Mammography by far has been the most successful and has demonstrated in many studies that by diagnosing minimal cancer it can result in curing the disease.[3] However, mammography has not effectively reduced the mortality rate in the United States[1] and has problems such as a false negative rate of 15%–20%, an overall specificity of 50% and high false positive rates because both malignant and benign tumors appear similar at an early stage,[4] questionable effectiveness in detecting tumors in young women with dense breasts, a wide variability in the technical aspects of taking the x-rays and in the expertise of those reading the films. To minimize false images produced by overlying tissue, the breasts are compressed during mammography. The resultant compression of the breast may cause a cyst to rupture in the breast and mass may disappear from the mammogram.[5] Differentiation of lesions such as fat necrosis or lipomas from malignant ones has been a difficult task. Ionizing radiation of x-ray mammography is considered a biohazard, particularly in younger patients[6] due to repetitive imaging. Because of the considerable time necessary to x-ray a single subject and to read the mammogram, it is also questionable whether or not it could realistically be used to annually examine the 65 000 000 women who need studying.

Based on light absorption phenomena by a solid mass in breast, transillumination techniques have been investigated and have demonstrated the shadow of a solid mass.[7] Although this technique can detect and visualize breast tumors noninvasively and noncontact, further developments should be done to detect small tumors.[8] Because conventional transillumination techniques have limited sensitivity and specificity, when compared to x-ray mammography, a new technique has been proposed to enhance the contrast of tumors. Total time of photon travel into breast tissue is measured by a direct time-of-flight measurement and phase detection of intensity modulated laser beam. This technology is called the frequency-domain approach.[9] Even though frequency-domain laser

Address all correspondence to Daniel B. Sheffer. Tel: 330-972-6650; Fax: 330-374-8841; E-mail: r1dbs@brain.biomed.uakron.edu

scanning mammography (FLM) could improve sensitivity and specificity, further study must be done to overcome detection sensitivity issues at or around the edges of the breast.

In the early stage of cancer, the growing number of cancerous cells causes hypercellular and possibly desmoplastic response.[10] The epithelium of a mammary duct with a primary carcinoma changes very rapidly and extensively, as the layer thickens.[11] As cancerous cells grow and spread, dermal layers have more lymphatic or collagenous deposition and resultant skin edema becomes apparent, so skin thickness reaches approximately ten times that of normal.[12,13] Therefore not only malignant, but other tissues have additional mass or density and thus change the biomechanical properties of breast tissue.[13] We have attempted to detect the changes in breast by examining the tissue mechanical response to pressure or vibration stressing. For the detection of the mechanical response of breast tissue, we used holographic interferometry (HI) which is a noninvasive and noncontact modality for possible use in routine breast cancer screening.

The HI technique has been successfully used in industry for nondestructive testing of structural defects of laminate materials.[14] When a holographic film is exposed twice during the relaxed and deformed states of an object by either pressure or vibration stressing, interference fringes are created. Equal amounts of displacement are represented by a continuous and uniform fringe pattern. A distinctive fringe density or aberrant pattern in reconstructed images represents sudden and localized deformations.

Application of the HI technique to either isolated biological tissues or a human subject has been reported by some investigators[15,16] to be a very sensitive imaging technique. When the object beam is shifted by deformation of an object by θ, between two exposures, the resultant fringe line spacing, D, on the interferogram is given by[17]

$$D = \frac{n\lambda}{2\sin(\theta/2)}. \tag{1}$$

When n and λ indicate the index of refraction and wavelength, respectively, if the object beam angle difference, θ, is minimal, approximately 0.5°, and the pulsed Ruby laser has a wavelength of 694 nm, the displacement, D, would be $1.0\times 694\times 10^{-9}/(2\times\sin(0.25))\approx 80\,\mu$m between two fringe lines, which suggests that a tumor which is not easily detectable by physical exam or mammography can result in a sufficiently large and distinctive local deformation to cause noticeable fringe distortion. Involuntary movement such as breathing and vibrations of the thorax due to the cardiac cycle of a subject and environmental disturbances have been limiting factors in the application of a cw laser for HI technique. To address this problem, we employed a pulsed ruby laser with a pulse width of 30 ns and a pulse interval ranging from 200 through 800 ms.

Following experiments performed in our laboratory, we found that vibration and pressure stressing techniques appeared to be appropriate and effective, producing adequate fringe density and contrast.[18–20] Vibration stressing delivered strain energy deep into the breast tissue and resulted in fringe distortions which were clearly visible around a localized tumor.[18] However, detection of fringe distortion associated with lesions was highly dependent on the location of the vibration source when applied to the surface of subject's breast or thorax.

Hydraulic and pneumatic pressure applications were studied as alternative stressing modalities. Hydraulic pressure was created when air filled bladders were expanded to raise the water level within the Plexiglas chamber thereby compressing the subject's breasts.[19] The resultant hydraulic pressure was uniform and produced well-defined and concentric fringe patterns on the apex of the breast which was dependent in the chamber. However, some drawbacks were noted. (1) For cleanliness, the water within the chamber had to be changed for each subject. (2) Water turbulence or tiny air bubbles and chemical particles caused laser beam scattering and speckle on a hologram image. To overcome these limitations a pneumatic pressure system was designed and tested. Two opposing plungers were attached to the sidewalls of the Plexiglas chamber which could reduce the internal volume of the chamber and create a changing pneumatic pressure. The plunger motion was precisely computer controlled so that stressing parameters, such as the amplitude and frequency of pressure variation, could be precisely modified for each subject to apply effective strain energy to the breasts. Even though airtight sealing around the subject's thorax was a difficult task, the degree of sealing and uniformity of pressure within the chamber could be verified through a prosthetic model and subject experiments. In this paper, the pneumatic pressure stressing is examined and discussed.

2 MATERIALS AND METHODS

The instrumentation for production of HI consists of optical and computer based controlled subsystems. The optical subsystem includes an optical setup to take a hologram and the supporting electronics for the pulsed ruby laser. The computer-based controller (CBC) includes the electronics necessary to create the plunger driving signal, delay registers to control the timing of the laser firing and plunger motion. The laser power unit is also controlled by this subsystem.

The optical setup for holography consisted of a pulsed ruby laser holocamera (JK Laser, HLS-2) producing a total of 1 J of energy at a wavelength of

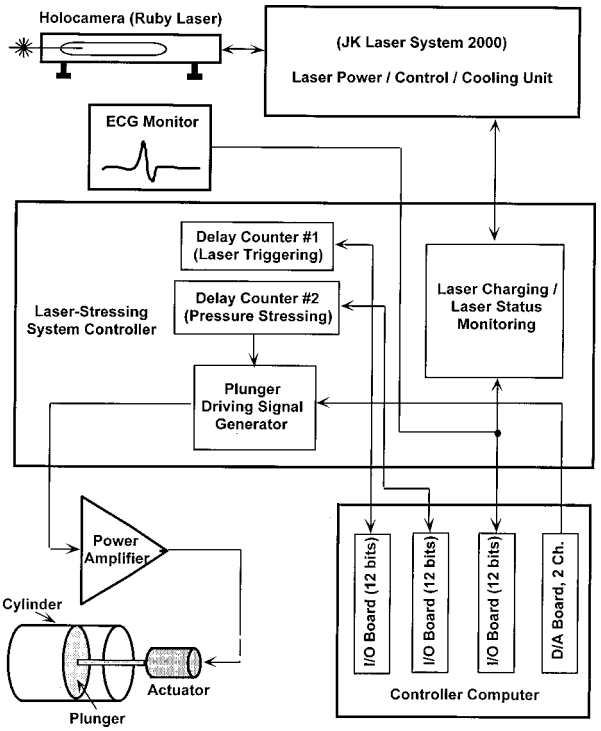

Fig. 1 Schematic diagram of holographic interferometry system: The pulsed ruby laser unit, computer based controller (CBC), and pressure generating unit are shown in this diagram. Laser firing is controlled by a complementary metal-oxide semiconductor (CMOS) level signal (+12 V) coming out of an electronic circuit board installed within the CBC. Actual setup of an actuator and a plunger is shown in Figure 2.

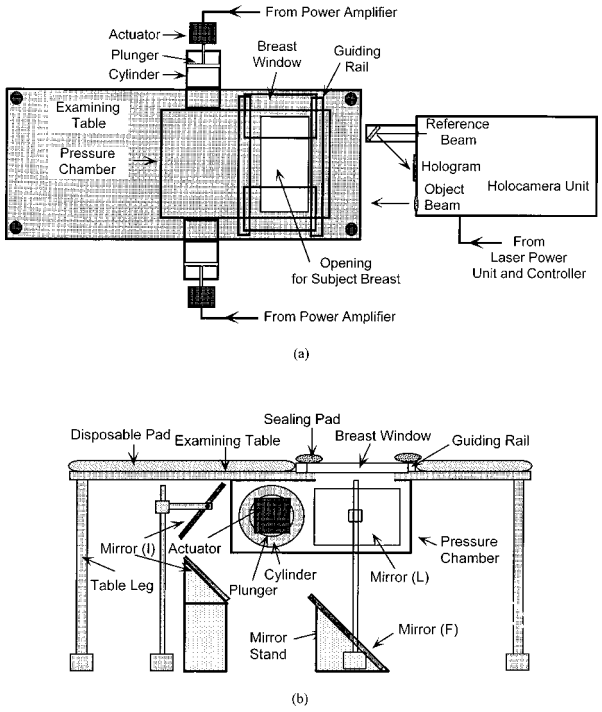

Fig. 2 Experimental setup of holocamera and examining table: (a) The top view of the entire system layout is shown. The laser control unit is a separate unit from an examining table. The holocamera control electronics and power amplifier for the two plungers are mounted in a mobile rack. (b) A side view of the examining table with its pressure chamber, in which the object beam mirrors are shown. When a subject is lying on an examining table, both breasts hang naturally within the pressure chamber. Two plungers move laterally at both sides of a pressure chamber. The examining table is made of a block of lucite (787 mm×2184 mm) with a thickness of 16 mm. It was designed to prevent air leakage and to allow easy adjustment of optics beneath the examining table. Physical dimension of the pressure chamber is 533 mm (W) ×406 mm (H)×254 mm (D). Diameter of the plunger is 152 mm. The opening of an examining table is 305 mm (W)×203 mm (H).

694 nm. By Q-switching the laser cavity, double pulses are created with an interval of 200–800 μs between pulses. The beam coming from the ruby amplifier is split into an object and a reference beam necessary for holographic recording.

The CBC and connected subsystems are shown in Figure 1. The host computer controller takes both digital and analog signals through the input–output (I/O) boards. The CBC initiates charge of the capacitor in triggering the flash lamps within the laser cavity and monitors the holding voltage. With a keyboard input, Q switching is activated and thus the pulsed laser beam is released from the holocamera. As the two plungers attached to the opposing lateral sides of the chamber move, the pressure within the chamber changes (Figure 2). The chest wall of the subject forms one wall of the chamber through an opening in the examining table (Figure 2), and therefore the subject's breasts are exposed to the internal pressure changes within the chamber. According to optimum protocols saved in computer memory, the computer controls the timing interval between the pressure stressing signal and laser triggering by setting three delay counters and thus takes double exposed hologram when the subject's breasts are mildly deformed, resulting in appropriate fringe contrast and density. Judicious selection of the optimum protocols is made using empirical data classified by the subject's cup size, which is indicative of the mass of the breast parenchyma, and easily obtainable data by querying the subject: A, B, C, D, and E (see Table 1 and Sec. 3). The pro-

Table 1 Optimum protocol for each cup size: The parameters to control a plunger driving signal and laser pulse interval are shown for each cup size. Twenty four holograms were taken to finalize the optimum parameters for each cup size.

Subject's cup size	Laser pulse interval [μs]	Amplitude	Frequency	Phasing
A	400	Low	5	Negative
B	400	Low	5	Positive
C	400	Low	5	Positive
D	400	Low	5	Positive
E	800	High	10	Positive

file of internal pressure within the chamber is determined by modifying the amplitude and/or frequency of the plunger driving signal, which is programmed by the CBC. Because low pressure levels (maximum 14 mm H_2O) are used to deform the subject's breasts, the temperature within the chamber is assumed to be constant; therefore, the pressure, P', created by plunger motion is given by

$$P'(t) \approx \frac{V_o}{V_o - \pi R_p^2 L_p (A_s/5[\text{volts}])\sin(2\pi f_s t)} P_o, \tag{2}$$

where V_o, R_p, A_s, f_s and P_o represent, respectively, the initial chamber volume, radius of the plunger (76 mm), the amplitude (volts) and frequency of plunger displacement (sinusoidal) [Hz] and the initial pressure within a chamber. The L_p, maximum stroke length of a plunger, is 46 mm. As Eq. (2) shows, the amplitude and frequency of a plunger driving signal are the controllable effects of the rate of pressure change. In the CBC, the wave form for the plunger driving signal is determined by two parameters, the amplitude, A_s, and the frequency, f_s, which were programmable and set according to the optimum stressing protocol for each cup size (see Table 1). To minimize the minute vibration due to plunger recoil motion, the plunger position is precisely monitored by a linear position sensor and controlled by the CBC. The pressure signal, $P'(t)$, is monitored in real time by a piezoresistive pressure sensor (Motorola, MPX10) mounted on one side panel of the chamber.

Because HI can detect small displacements, it has been used to detect chest wall vibrations for studying cardiovascular function.[16] However, in this study, chest wall vibration originating from either cardiac apex motion or respiration of a subject causes additional nonuniform fringes.[18] Therefore, the CBC was designed to include circuitry interfaced to an ECG (electrocardiography) monitor (Hewlett-Packard, 78390A) to detect a subject's ECG signal. Once detected, the CBC starts a master clock thus creating the stressing signal and triggering the laser after an appropriate delay time to minimize the cardiac effect. The CBC circuitry detects transistor–transistor logic (TTL) compatible *R*-wave (ventricular depolarization) signals from the ECG monitor, and then acquires the *R*-wave pulse train and calculates the average cardiac cycle length for up to 20 cycles. As a rule of thumb, unless a patient demonstrates bradycardia or tachycardia, the time at 70% of the cardiac interval between the *T* wave (ventricular repolarization) and subsequent *P* wave (atrial depolarization), is selected as the laser delay time. The detailed structure of the CBC program is shown in Table 2.

The subject is asked to lie on an examining table in the prone position. The relative position of the examining table to the holocamera is shown in Figure 2. Both breasts are hanging naturally within the Plexiglass pressure chamber so that the base of the breasts is pulled away from the axilla. To prevent air leakage and provide a comfortable setting for the subject's chest wall on the examining table, a silicon pad (New Pig Corporation, PLR201) is placed around the edges of the breast chamber window. The edges of the breast window are also wrapped with padding for the subject's comfort and to further maintain an airtight seal.

The center of the hologram is aligned to the center of the opening in the examining table. The direction of an object beam leaving the holocamera is simply adjusted by moving the beam-expanding lens. Using an in-line HeNe laser spot, the resulting beam of pulsed ruby light is directed toward the center of a subject's sternum. Beneath the examining table, five sets of mirrors are installed to provide coverage of all views of the breasts: superior, frontal, left, right, and inferior (Figure 2). Each view is easily obtained from one hologram and recorded by a video camera (Panasonic, model WV 1550) and a frame grabber (Data Translation, model DT2867).

The exposed holographic films (AGFA, model 8E75HD-4) are developed (Kodak D-19, developer) for 3–6 min and fixed (Kodak, Undiluted Rapid Fixer without hardener) for 5 min. Water stains on the developed film are removed (Kodak, Photoflo). The film is air dried for at least 30 min before image reconstruction. The holographic image is reconstructed using a 30 MW HeNe laser (Siemens, model LGK 7626). The angle of the reconstruction beam to the holographic film is set at 52.6° with respect to the film plate. A schematic of the setup for image reconstruction is shown in Figure 3. With a video camera and a frame grabber (Data Translation, model DT2867), the reconstructed image is imported into a computer for further image processing.

3 RESULTS AND DISCUSSION

From Eq. (2), it is clear that surface deformation is proportional to the degree of stressing and should be enough to clearly show localized and distinctive patterns due to an underlying lesion. Experiments were performed to determine optimum stressing protocols for different masses of breast parenchyma, i.e., cup size. With combinations of parameters selected to control fringe density, amplitude and frequency of the plunger driving signals, and the laser pulse interval, 24 holograms were taken for each cup size. The following parameters were modified for the recording of each hologram to find the best fringe pattern in the image: the laser pulse intervals of 200, 400, 600, and 800 μs, stressing phase, i.e., positive or negative pressure, amplitude of plunger driving signal: high (2.2 V), low (1.7 V), the frequency of driving signal: high (10 Hz) or low (5 Hz). Each image was carefully examined visually and the parameters producing images with a man-

Table 2 Structure of programs for computer based controller (CBC): Three major programs are listed according to their functions and input/output signals. The system operator runs the program PEDIT before calibrating laser and plunger motion controller or recording holograms. With program PEDIT, the optimum protocols for each cup size can be modified. The program, PROCAL is used for holographic recording of a prosthetic model and setting of parameters to control plungers. The program RECORD takes the ECG signal from a subject and triggers ruby laser according to the optimum protocol set and modified by the programs PEDIT and PROCAL. All of these three programs were written with Turbo C++ (V.3.0, Borland Co.).

Program name	Input	Function	Output
PEDIT (editing protocol)	(1) Cup size (A, B, C, D, E) (2) Number of frame (3) Plunger driving signal: amplitude, frequency, offset, stressing phase	Storing amplitude, frequency, initial position offset values to optimally control plungers	File containing optimum stressing parameters for each cup size (A, B, C, D, E)
PROCAL (protocol calibration)	(1) Amplitude, frequency, offset values (2) Delay times for laser and stressing control (3) Laser status signals (charging, ready, fired, failed to fire)	(1) Adjust the amplitude, frequency, and offset of a plunger signal according to the optimum protocol (2) Change delay times to control a plunger motion and laser firing (3) Fire ruby laser to check stressing phase (4) Drive the plungers to check the pressure level	(1) Save parameters of plunger driving signal (2) Issue a command to charge up the ruby laser
RECORD (recording holograms)	(1) Subject information; ID number, name, cup size, date of recording (2) Parameters from a file storing parameters of optimum protocol (PROCAL output file) (3) *R*-wave sync signal from ECG monitor (4) Operation status of laser	(1) Read optimized parameters for each cup size (2) Save the parameter values in the temporary memory of a computer (3) Read delay times for laser and stressing control (4) Save the delay values in temporary memory (5) Read the *R* wave to determine delay time of laser triggering and update the delay times for laser and stressing (6) Trigger the ruby laser	

ageable density of fringe lines and contrast were chosen as optimum protocols and were saved in a computer. Finalized optimum protocols for each cup size are shown in Table 1. For good quality of fringes, the optimum protocol for a small breast, size A, should be different from that used for a large breast, size E. For sizes, B, C and D, the same stressing protocol could be used.

Prior to applying the selected protocols on a human subject, experiments with a prosthetic model were performed and the results enabled satisfactory detection of abnormal profiles of fringe patterns around an inclusion.[18–20] In this paper, we are reporting results obtained with the computer-based controller (CBC) and five mirrors to cover five views of a subject's breast. Results are shown in Figures 4–8. Pneumatic pressure was used as the stressor to obtain those results.

At Summa Health System's Akron City campus, subjects were recruited from the regular mammography patient pool and from volunteers with known abnormalities in the breasts. The holographic images shown in Figure 4 were taken from a volunteer with a normal breast using the protocol for size B (Table 1). Five mirrors positioned as shown in Figure 2 obtained five different images. Density and contrast of fringe lines were deemed appropriate for screening abnormalities. As a result of numerous trials performed in our laboratory, it was determined that thorax asymmetry would not affect fringe patterns because the subject's breasts were naturally dependent due to lying on a prone position and uniformly exposed to chamber pressure during recording of a hologram. On the frontal image of the subject's breast, a concentric circular pattern of fringe lines was produced, which was an

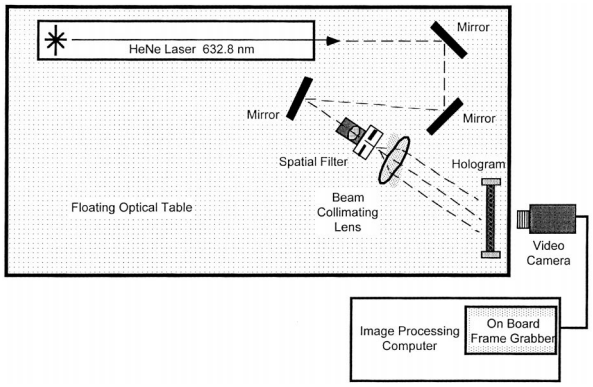

Fig. 3 Reconstruction of holographic image: The reconstruction setup shown above was installed on a floating optical table. The beam angle was adjusted to match that of the recording object beam. The plate holder and collimating lens were also adjusted for optimal contrast and brightness of reconstructed image. Holographic images were transferred to the image processing computer using a video camera and a frame grabber.

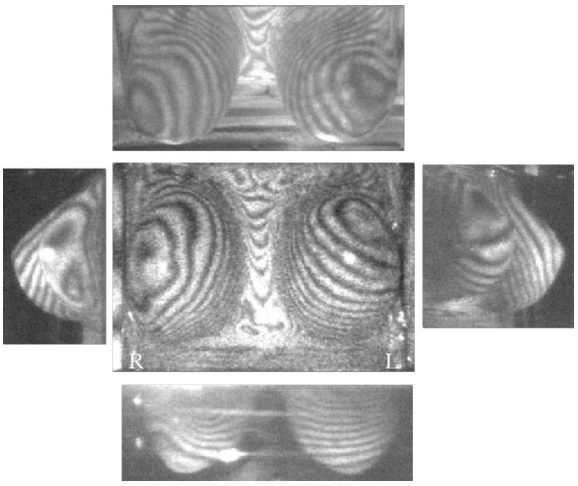

Fig. 5 Five holographic images of a normal subject (Stressing 1): A portion of the inner quadrant view is visible on two lateral views, right and left. This hologram was also taken from a subject with no known breast tumors.

evidence that uniform pressure was applied to the breast. This symmetrical pattern was also found around the xiphoid process and abdominal areas, because shadows were cast on the breasts by illumination of the object beam. The lateral views of holograms were generally dark. The inferior view is darker than the others because the object beam is attenuated more by the two reflecting mirrors (see Figure 2). Bright spots on the left upper corner of the frontal view and in the middle of an inferior view were due to the intense light emitted from the object beam-expanding lens. The sternal area in between both breasts is clearly visible.

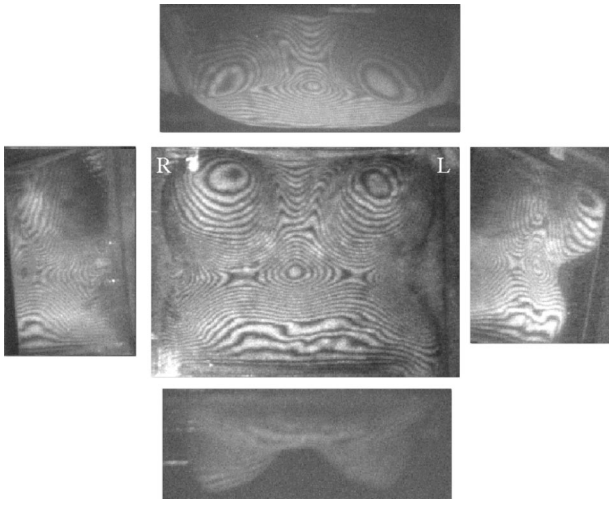

Fig. 4 Five holographic images of a normal subject: Five different views are captured from each hologram: superior (corresponding to cranio-caudal view of x-ray mammogram), two lateral, a frontal and an inferior views. R and L marked on the holographic images indicate right and left lateral aspects of the subject's thorax. The same definitions are used for Figure 8. Subjects of these holograms were known not to have any tumors in the breasts.

Other examples of holograms taken from subjects with normal breasts are shown in Figures 5 and 6. Because of the attenuation by mirrors and shadowing effects, the two lateral and inferior views are relatively darker compared to the frontal and superior ones. A bright spot and line in the inferior views were caused by laser beam reflections at the surface of mirror and the chamber wall. Figures 5 and 6 were recorded by two different stressing protocols from the same subject, 1.7 V of amplitude and 5 Hz for the frequency of the plunger driving signal, but Figure 6 was recorded at a pressure level 50% higher than that of Figure 5. The laser pulse interval was 800 μs for both holograms. Certainly, the higher pressure created higher density of fringe lines, while demonstrating a similar fringe pattern

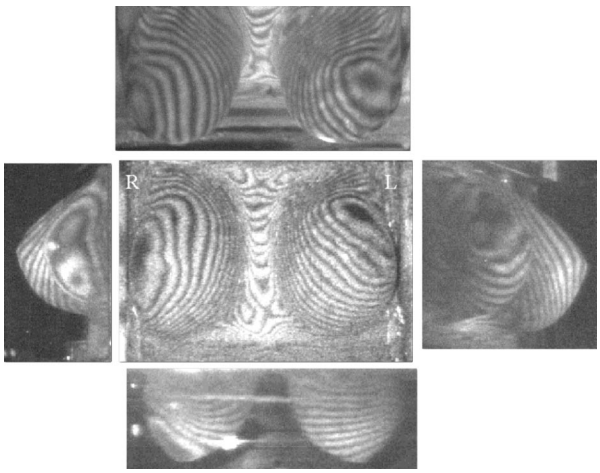

Fig. 6 Five holographic images of a normal subject (Stressing 2): These holograms are of the same subject shown in Figure 5, but with a different stressing protocol (50% higher pressure). Overall fringe pattern is similar to that in Figure 5, except for an increased density of fringe lines due to the higher pressure.

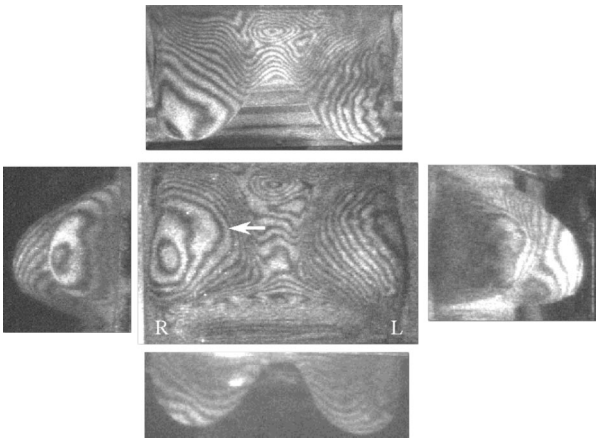

Fig. 7 Five holographic images of a subject with a nodular density in the breast (Stressing 1): These holograms were obtained from a subject with a nodular density on the upper inner quadrant of the right breast. On the superior view, well defined, regular and symmetric fringe patterns are visible around the sternum.

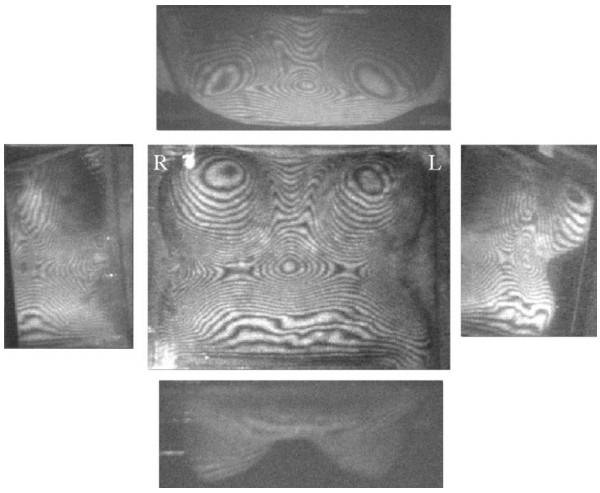

Fig. 8 Five holographic images of a patient subject with nodular density in the breast (Stressing 2): These holograms were also obtained from the same subject shown in Figure 7. However, the frequency of stressing signal (10 Hz) was twice that used in Figure 7. In the frontal view, low density and distortion of fringe lines are clearly visible at around the same suspicious area seen in Figure 7.

on both images. Slightly distorted fringe lines around the lower lateral quadrant of the right breast are due to the areola. This anatomical feature was also found in the images of a different subject shown in Figures 7 and 8. The nonsymmetrical pattern of fringes on both breasts was due to improper positioning of a subject on the examining table.

Holographic images obtained from the patient with a breast lesion are shown in Figures 7 and 8. Two holograms were recorded using several different stressing protocols for size D; In Figure 7, low frequency (5 Hz) and in Figure 8, high frequency (10 Hz) plunger driving signals were used. As Eq. (2) shows, a higher frequency plunger driving signal [i.e., higher f_s in Eq. (2)], produced a higher density of fringe lines because of a greater pressure gradient. Based on images previously recorded, there are typical patterns of fringe image abnormalities: (1) discontinuous fringe lines, (2) an isolated fringe line, (3) asymmetrical fringe patterns for both breasts, and (4) local changes in fringe density. The patient recruited for the recording seen in Figures 7 and 8 had a 4×6 mm nodular density on the right upper medial quadrant. This tumor was located on both holograms as belonging to fringe abnormality categories 3 and 4 mentioned above. The fringe patterns of both breasts are dissimilar and the fringe line density was suddenly reduced in the right breast. These abnormal signs of fringe lines are affected by the underlying breast structure and the direction of force applied to the surface of the breast. The site of the lesion shown in two x-ray mammograms (Figure 9) matched those associated with the fringe distortions shown in Figures 7 and 8.

As mentioned in the Introduction, it is known that both malignant and benign tumors result in local increase in density and/or mass of breast tissue, and cancerous tumors develop increasing mass by a hypercellular growth phenomenon. However, in x-ray mammography, visible changes of local density are not necessarily a direct sign of malignant tumor.[10] The system described in this report was also designed to detect both malignant and benign tumors according to those histologic changes. Therefore, the present system should be viewed as a screening tool for breast cancer, rather than a diagnostic procedure.

Cancerous cells are known to double 30 times until they become a size of 10 mm.[4,11] Therefore, the sensitivity requirement of this system was set to detect a nonpalpable tumor of size 10 mm or less. We have previously reported results, which have demonstrated the feasibility of detecting early stage cancer from experiments with both a prosthetic model

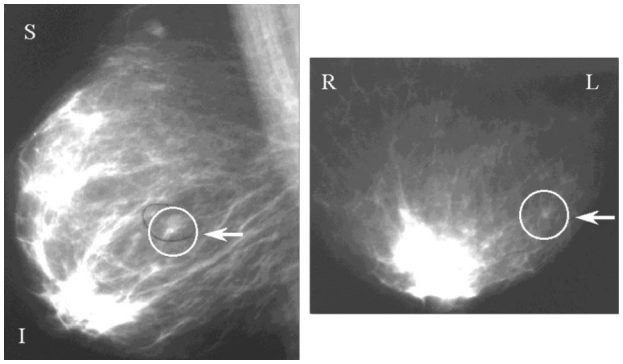

Fig. 9 Mammograms of subjects: This picture shows the x-ray mammogram of the subject seen in Figures 7 and 8. The mammogram on the left is a medial lateral view of the breast showing the location of the lesion in the right breast. A circle and an arrow indicate the site of the tumor. Part of the pectoralis muscle is visible. The marks, ''S'' and ''I'' represent the superior and inferior sides, respectively. The cranio-caudal view of a mammogram is shown on the left. R and L on the picture represent right and left lateral sides of the breast. An arrow and circle also show the location of the tumor.

and subject.[20,21] In the case of the prosthetic model, it contained an inclusion 5 mm in size which was made of epoxy glue. Fringe line distortion was clearly visible around an inclusion.[20]

In several cases, subjects had scars on the breast surface, which were due to previous lumpectomies or biopsies. At times, these scars resulted in local fringe line distortions, which were caused by localized tissue hardening. In these instances, fringe line distortions could be easily identified as to the cause and not selected as suspicious. Another possibility for false fringe line distortion may be due to an inflammation. Even though our subject pool did not contain subjects with inflammation, we hypothesize that these may also create false fringe line distortion depending on the hardness of the involved tissues. The HI technique used in the present study was examining the surface displacement of subject's breasts; and therefore if a tumor is not properly stressed by external pressure application, it may not cause a detectable local abnormality in surface displacement. This particularly may be true if a tumor is located deep inside and / or near the center of the breast parenchyma. We are currently performing a clinical study to investigate depth-dependent sensitivity of this system.

4 CONCLUSION

HI has been successfully used for material research in industry for the last 30 years. However, to our knowledge, this is the first attempt to apply the HI technique to breast tissue for the purpose of breast cancer screening. Preliminary results suggest that local fringe distortions caused by variation in the elasticity of underlying breast tissues could be found, which related to either increased breast tissue mass or hypervascularity caused by the angiogenesis during development of a tumor. Optimized protocols to properly stress and create a manageable density of fringes was developed for different masses of breast tissue. If not controlled, subject motion, the nonplanar and nonuniform shape of the chest wall could result in nonrepeatable fringe patterns from the same subject. As demonstrated, we obtained repeatable fringe patterns from the same subject using the CBC system. Further studies include development of devices to improve performance of the stressing mechanism, to deliver object beam efficiently without causing shadows on the lateral breast images and to unwrap the phase of fringe lines for automated analysis of abnormalities in the breast tissue.

Acknowledgments

The authors would like to acknowledge the invaluable contribution of our subject volunteers for this project. Brynna Baird, a graduate student at the University of Akron, is acknowledged for her excellent efforts in fabrication of the control system, recruiting patients, and conducting the data acquisition. We also acknowledge the technical expertise of Dick Henry, Grant Jungen, and Rick Nemer from the University of Akron and Patricia Robinson of Akron City Hospital. The Summa Health System Foundation (Charles H. Loughry Cancer Fund) Akron City and the University of Akron supported this study.

REFERENCES

1. J. C. Bailar and H. L. Gornik, ''Cancer undefeated,'' *N. Engl. J. Med.* **336**(22), 1569–1574 (1997).
2. S. H. Landis, T. Murray, S. Bolden, and P. A. Wingo, ''Cancer statistics, 1998,'' *CA Cancer J. Clin.* **48**(1), 6–30 (1998).
3. S. A. Feig, ''Decreased breast cancer mortality through mammographic screening: Results of clinical trials 1,'' *Radiology* **167**, 659–665 (1988).
4. *Breast Diseases*, J. R. Harris, S. Hellman, I. C. Henderson, and D. W. Kinne Eds., Chap. 5, J. B. Lippincott, Philadelphia (1991).
5. D. R. Pennes and M. J. Homer, ''Disappearing breast masses caused by compression during mammography,'' *Radiology* **165**, 327–328 (1987).
6. R. H. Mole, ''The sensitivity of the human breast to cancer induction by ionizing radiation,'' *Br. J. Radiol.* **51**(606), 401–405 (1978).
7. R. J. Bartrum and H. C. Crow, ''Transillumination light scanning to diagnose breast cancer: A feasibility study,'' *Am. J. Roentgenol.* **142**, 409–414 (1984).
8. A. Alveryd, I. Andersson, and K. Aspegren, ''Light scattering versus mammography of the detection of breast cancer in screening and clinical practice,'' *Cancer (N.Y.)* **65**, 1671–1677 (1990).
9. K. T. Moesta, S. Fantini, H. Jess, S. Totkas, M. A. Franceschini, M. Kaschke, and P. M. Schlag, ''Contrast features of breast cancer in frequency-domain laser scanning mammography,'' *J. Biomed. Opt.* **3**(2), 129–136 (1998).
10. R. C. Cory and S. S. Linden, ''The mammographic density of breast cancer,'' *Am. J. Roentgenol.* **160**, 418 (1993).
11. H. S. Gallager and J. E. Martin, ''Early phases in the development of breast cancer,'' *Cancer (N.Y.)* **24**(6), 1170–1178 (1969).
12. H. S. Shukla, L. E. Hughes, L. H. Gravelle, and A. Satir, ''The significance of mammary skin edema in noninflammatory breast cancer,'' *Ann. Surg.* **189**(1), 53–57 (1979).
13. M. M. Black, F. D. Speer, and S. R. Opler, ''Structural representations of the tumor-host relationships in mammary carcinoma, Bologi and prognostic significance,'' *Am. J. Clin. Pathol.* **26**, 250–257 (1956).
14. R. K. Erf, *Holographic Nondestructive Testing*, Academic Press, New York (1974).
15. A. Hofstetter, R. Bowering, E. Keiditsch, and H. Wachutka, ''Interferometric laser holography for determination of the localization and extent of bladder tumor,'' *Eur. Urol.* **5**, 120–127 (1979).
16. S. M. Yivi and G. H. Humberstone, ''Chest motion visualized by holographic interferometry,'' *Med. Res. Eng.* **9**, 5–10 (1970).
17. G. B. Brandt, ''Holographic Interferometry,'' in *Handbook of Optical Holography*, H. J. Caulfield, Ed., Chap. 10, Academic Press, New York (1979).
18. J. Woisetschlager, D. B. Sheffer, H. Mikati, and K. Somasundaram, ''Breast cancer detection by holographic interferometry,'' *Proc. SPIE* **1756**, 176–183 (1992).
19. J. Woisetschlager, D. B. Sheffer, C. W. Loughry, K. Somasundaram, S. K. Chawla, and P. J. Wesolowski, ''Phase-shifting holographic interferometry for breast cancer detection,'' *Appl. Opt.* **33**(22), 5011–5015 (1994).
20. H. D. Hong, D. B. Sheffer, and C. W. Loughry, ''Holographic interferometry for detection of breast lesion,'' *Proc. SPIE* **3011**, 121–130 (1997).
21. H. D. Hong, D. B. Sheffer, and C. W. Loughry, ''Holographic interferometry for early detection of breast cancer,'' *Int. Conf. IEEE EMBS* **18**, 580–581 (1996).